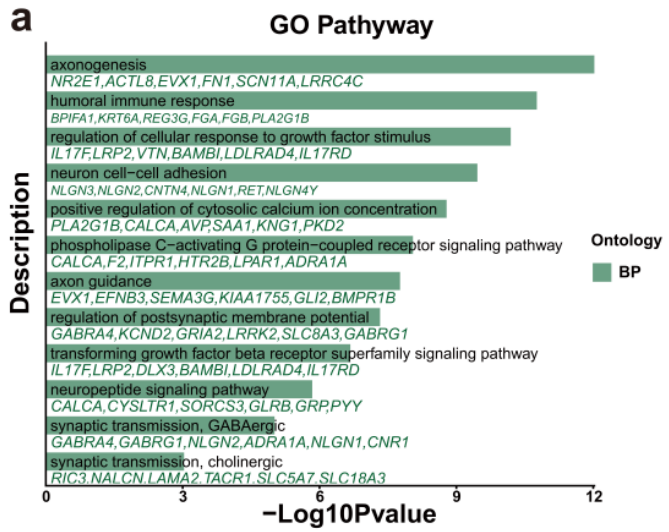
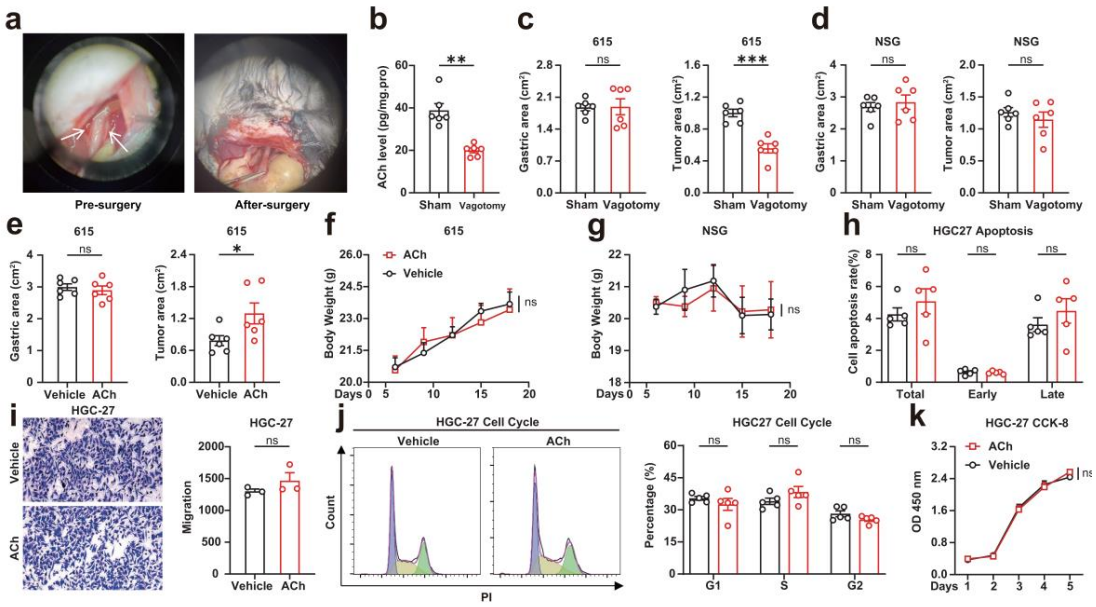


Extended Data Fig. 1. GO pathway enrichment analysis of PNI-associated tumors.

(a) GO pathway enrichment analysis revealing differentially activated pathways between PNI-high and PNI-low gastric tumors.



Extended Data Fig. 2. Characterization of the vagotomy model and the effects of ACh on gastric cancer progression.

(**a**) Representative photographs of the dissected vagus nerve (indicated by arrows) before (**a**, ***left***) and after (**a**, ***right***) subdiaphragmatic vagotomy.

(**b**) ACh concentrations in GC tissues from sham and vagotomy groups, measured by ELISA (*n* = 6).

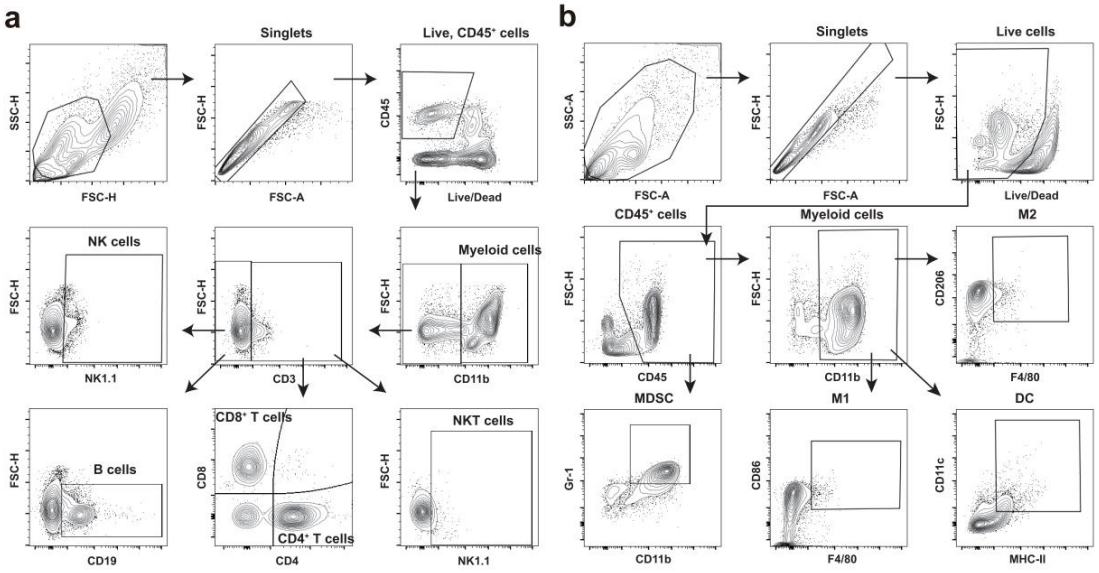
(**c–e**) Quantification of gastric area (***left***) and tumor area (***right***) across distinct orthotopic gastric tumor models. Cohorts include: immunocompetent 615 mice subjected to subdiaphragmatic vagotomy or a sham operation (**c**); immunodeficient NSG mice subjected to vagotomy or a sham operation (**d**); and immunocompetent 615 mice treated with exogenous ACh or PBS vehicle (**e**) (*n* = 6 mice per group).

(**f–g**) Body weight monitoring of mice treated with ACh in the MFC syngeneic model (**f**) and immunodeficient model (**g**) (*n* = 6 mice per group).

(**h–k**) *In vitro* assays of HGC-27 cells following ACh treatment (*n* = 3–6). Apoptosis assay (**h**); migration assay (**i**); cell cycle assay (**j**); CCK-8 cell viability assay (**k**).

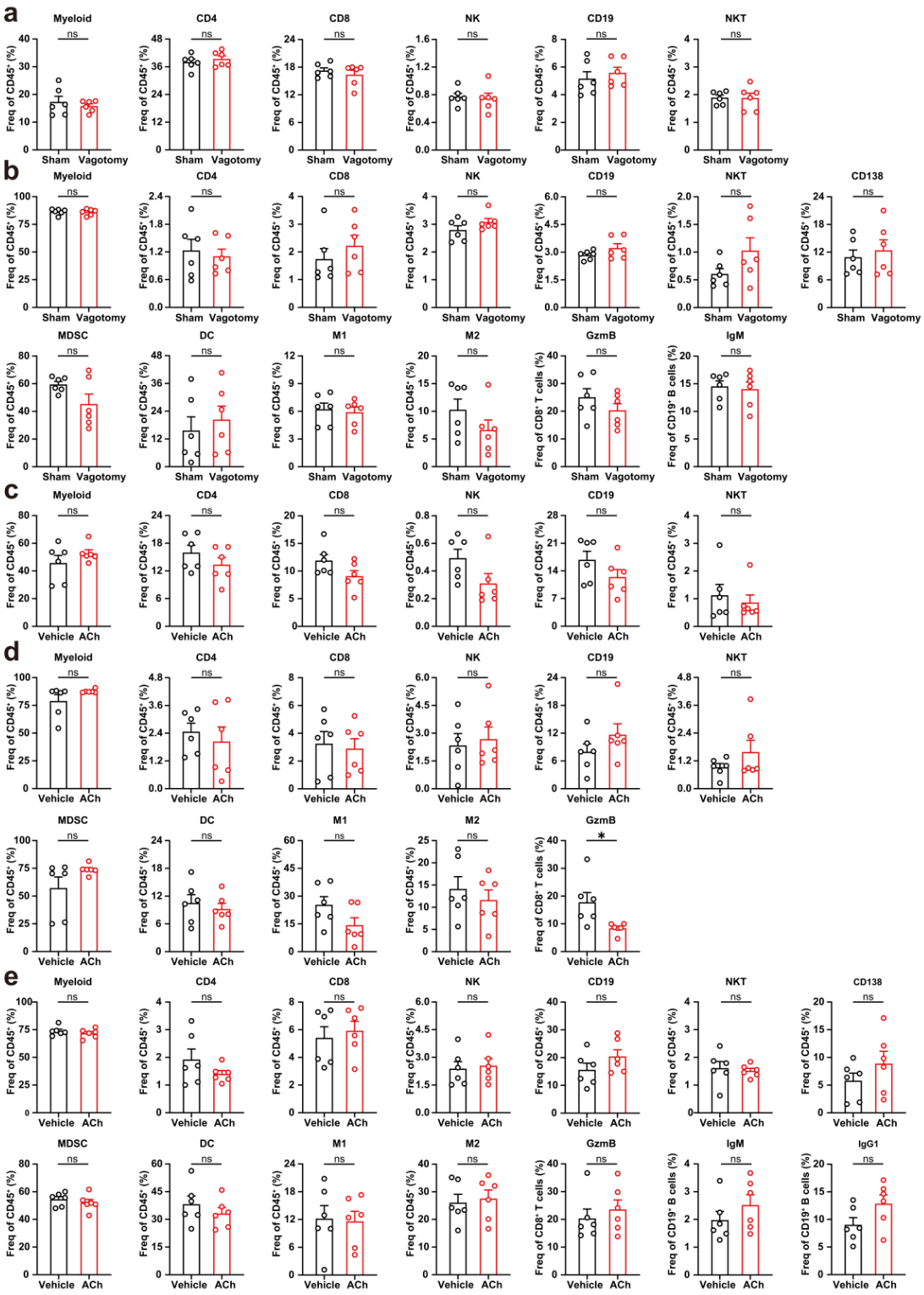
Statistical significance was calculated by unpaired two-tailed Student's t tests (**b, c, d, e, i**), one-way ANOVA (**h, j**) and two-way ANOVA (**f, g, k**). Error bars

represent SEM. * $P < 0.05$, ** $P < 0.01$, *** $P < 0.001$, and ns, not significant.



Extended Data Fig. 3. Flow cytometry gating strategies.

(**a–b**) Representative gating strategies for the identification and characterization of murine immune cell subsets.



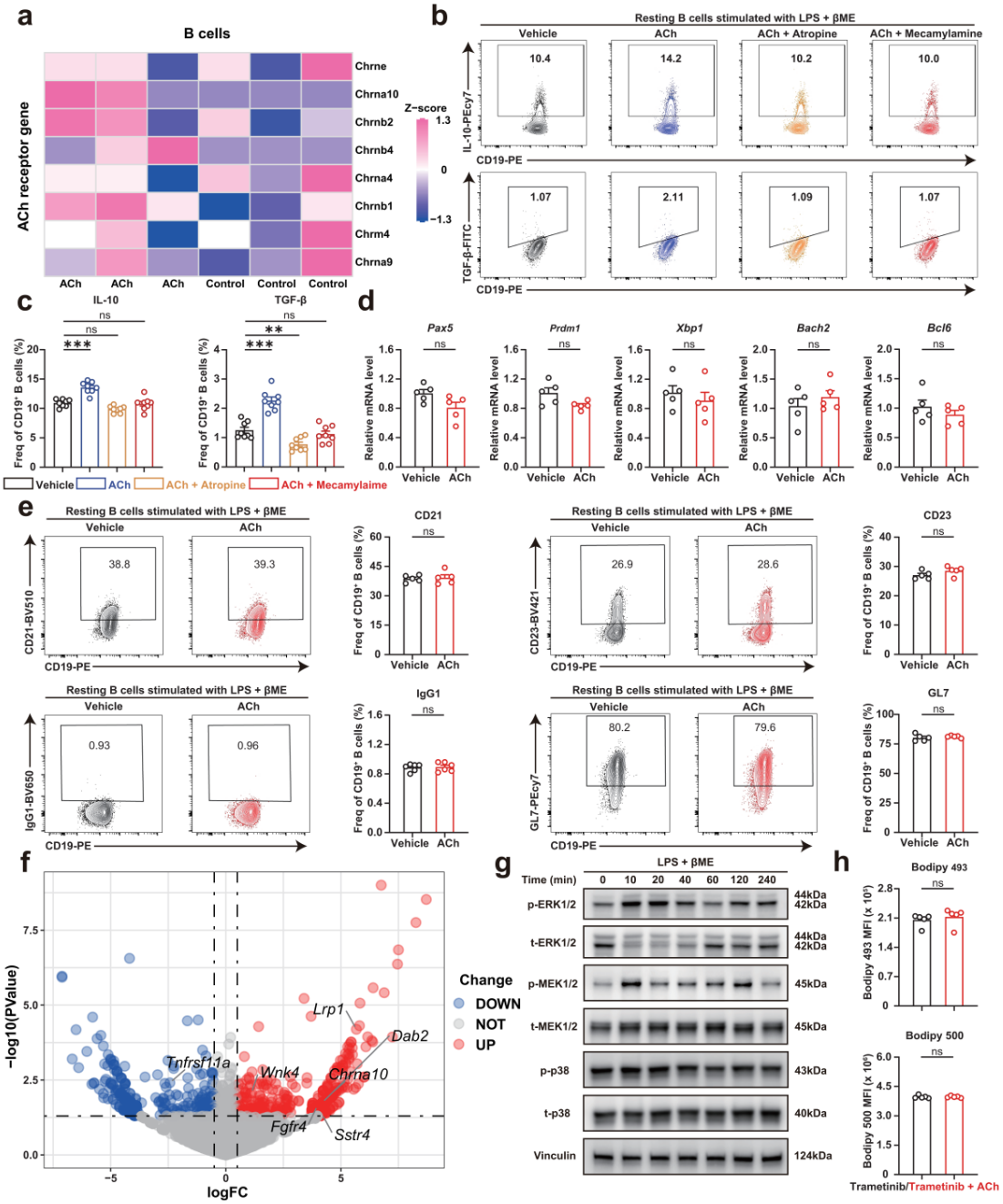
Extended Data Fig. 4. Profiling of systemic and local immune landscapes in syngeneic murine models.

(**a–b**) Flow cytometric analysis of immune cell subpopulations in the peripheral blood (**a**) and local tumor microenvironment (**b**) of the 615 syngeneic orthotopic tumor model, comparing sham vs. vagotomy groups (*n* = 6 mice per group).

(**c–d**) Flow cytometric analysis of immune cell subpopulations in the peripheral blood (**c**) and local tumor microenvironment (**d**) of the 615 syngeneic orthotopic tumor model, comparing vehicle vs. ACh groups (*n* = 6 mice per group).

(**e**) Flow cytometric quantification of tumor-infiltrating immune cell subsets in immunocompetent 615 mice bearing syngeneic subcutaneous tumors, comparing vehicle vs. ACh treatment groups (*n* = 6 mice per group).

Statistical significance was calculated by unpaired two-tailed Student's t tests (**a, b, c, d, e**). Error bars represent SEM. * $P < 0.05$, ** $P < 0.01$, *** $P < 0.001$, and ns, not significant.



Extended Data Fig. 5. Phenotypic, transcriptomic, and metabolic alterations in B cells following ACh stimulation.

(**a**) Relative mRNA expression of acetylcholine receptors in B cells treated with ACh or PBS, determined by bulk RNA-seq.

(**b–c**) Murine B cells were stimulated with LPS for 24 h and subsequently treated with or without 50 μM ACh, 10 μM Atropine or 10 μM Mecamylamine. The proportions of IL-10- and TGF-β-producing $CD19^+$ B cells were determined by flow cytometry (n = 8).

(**d**) Relative mRNA expression levels of *Pax5, Prdm1, Xbp1, Bach2* and *Bcl6* in murine B cells treated with 50 μM ACh or PBS for 24 h, determined by qRT-PCR (n = 5).

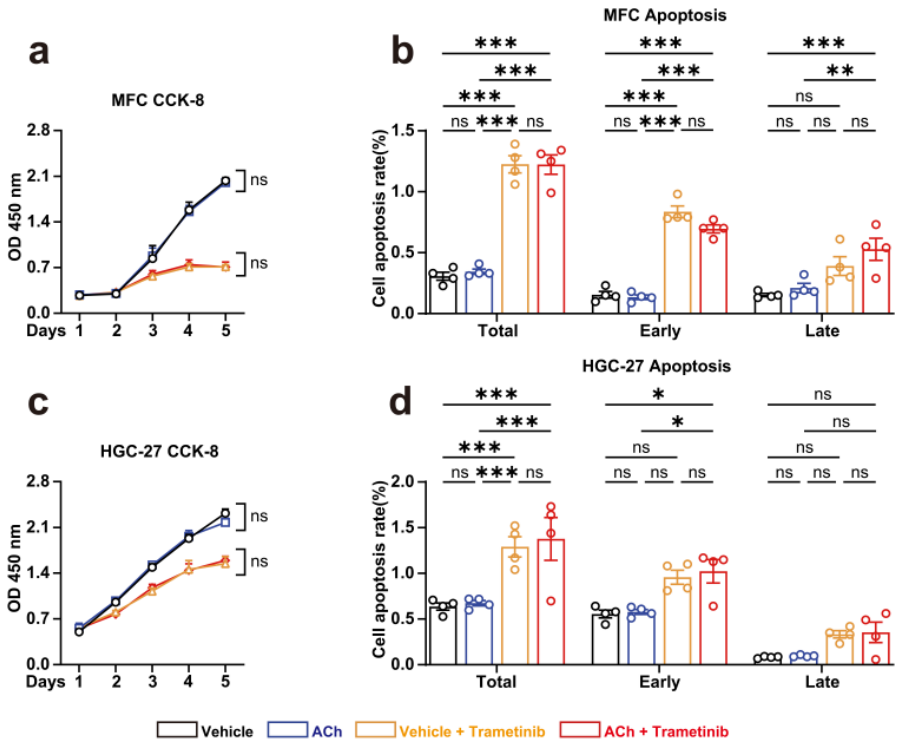
(**e**) Flow cytometric analysis of CD21, CD23, IgG1 and GL7 expression on murine B cells treated with 50 μM ACh or PBS for 24 h (n = 5).

(**f**) Volcano plot showing differentially expressed genes (DEGs) in murine B cells treated with ACh versus PBS.

(**g**) Immunoblots for indicated proteins of whole-cell lysates from B cells treated with ACh for the indicated times.

(**h**) Flow cytometric analysis of cellular lipid uptake and content in murine B cells. Cells were pre-treated with 10 μM trametinib for 30 min, followed by a 24-h stimulation with or without 50 μM ACh (n = 5).

Statistical significance was calculated by unpaired two-tailed Student's t tests (**d, e, h**) and one-way ANOVA (**c**). Error bars represent SEM. * $P < 0.05$, ** $P < 0.01$, *** $P < 0.001$, and ns, not significant.



Extended Data Fig. 6. Cell viability and apoptosis analyses of MFC and HGC-27 cells following ACh and trametinib treatment.

(**a–d**) In vitro evaluation of cell viability (via CCK-8 assay) and apoptosis in MFC (**a, b**) and HGC-27 (**c, d**) cells following exposure to ACh and/or trametinib (*n* = 4–6).

Statistical significance was calculated by two-way ANOVA (**a, b, c, d**). Error bars represent SEM. * $P < 0.05$, ** $P < 0.01$, *** $P < 0.001$, and ns, not significant.